Eur. Phys. J. B **26**, 229–234 (2002)
DOI: 10.1140/epjb/e20020084

THE EUROPEAN PHYSICAL JOURNAL B
EDP Sciences

Effect of positional disorder in systems of ultrafine ferromagnetic particles

M. Porto[a]

Max-Planck-Institut für Physik komplexer Systeme, Nöthnitzer Strasse 38, 01187 Dresden, Germany

Received 28 November 2001

Abstract. A simple model for systems of dipolarly interacting single-domain ultrafine ferromagnetic particles is studied by Monte Carlo simulations of zero field cooling and field cooling as well as relaxation experiments. By investigating systems characterized by an identical moderate concentration but different types of particle positions' disorder, it is shown that the positional disorder has a crucial influence on the magnetic behavior of the system. For extreme values of positional disorder, the interplay between spatial disorder and dipolar interaction can even lead to a cooperative freezing at low temperatures.

PACS. 75.50.Tt Fine-particle systems; nanocrystalline materials – 75.40.Mg Numerical simulation studies – 75.50.Lk Spin glasses and other random magnets

1 Introduction

The interplay of randomness and dipolar interaction has been intensively investigated in systems of single-domain ultrafine ferromagnetic particles (see Ref. [1] for a recent comprehensive review). Nevertheless, in difference to the well understood dilute systems [2–6], the experimental results for dense systems and their interpretation are still a matter of controversy [1,7–22]. In particular, there is little agreement concerning the existence and the origins of a spin glass phase at low temperatures. The signatures of a spin glass phase (such as a peak in the non-linear susceptibility at and aging phenomena below the transition temperature) have been reported for a variety of systems, for example for dense samples of γ-Fe_2O_3 [14], ϵ-Fe_3N [20], and amorphous $Fe_{1-x}C_x$ [21], but are absent in others. Additionally, it is not clear whether the experimentally observed spin glass behavior can be attributed to the interplay between random anisotropy and dipolar interaction, as conjectured in [13], or if the particles' spatial arrangement dominate the system's behavior, as pointed out in [22]. Intense theoretical investigations of diverse model systems (see likewise Ref. [1] for a comprehensive review) have not been able to resolve this controversy, as no ingredient could be identified as the crucial one leading to spin glass behavior [23]. These contradicting results get even more confusing, since it is known that disordered dipoles can indeed show a cooperative freezing in systems such as dipolar glasses [24]. So the crucial question has remained, if and under which conditions the interplay of randomly oriented anisotropies, spatially disordered particle positions, and dipolar interaction in systems of single-domain ultrafine ferromagnetic particles leads to a spin glass phase at low temperatures.

When comparing dipolar glasses with systems of single-domain ultrafine ferromagnetic particles, one notices that a major difference between the two classes of systems is the type of positional disorder. And indeed, the influence of the positional disorder in systems of single-domain ultrafine ferromagnetic particles has not been studied theoretically in much detail so far. To address the question whether certain types of particle positions' disorder might be the crucial ingredient leading to spin glass behavior, and to study the influence of positional disorder in general, extensive MC simulations of the model investigated in [23] using zero field cooling (ZFC) and field cooling (FC) as well as relaxation experiments are performed. By studying systems characterized by an identical moderate concentration but different types of particle positions' disorder, it is shown that the positional disorder has a large influence on the system dynamics. Therefore, the detailed characteristics of the spatial arrangement of the particle positions are found to be important for understanding and describing systems of single-domain ultrafine ferromagnetic particles. For extreme values of positional disorder, the system dynamics might even be interpreted as characteristic of cooperative freezing. This presumable spin glass behavior occurs, however, for parameter values which are not realized in the experiments for which spin glass behavior have been reported.

2 Model

Analogously to the model studied in [23], it is assumed here that every particle i consists of a single magnetic

[a] e-mail: porto@mpipks-dresden.mpg.de

domain with all its atomic moments rotating coherently, resulting in a constant absolute value $|\boldsymbol{\mu}_i| = M_\mathrm{S} V_i$ of its total magnetic moment $\boldsymbol{\mu}_i$. Here, V_i denotes the volume of particle i, and M_S is the saturation magnetization which is supposed to be independent of particle volume and temperature. The energy contribution of each particle i is composed of three parts: the anisotropy energy $E_\mathrm{A}^{(i)}$ (either caused by the particle's shape or crystalline structure), the field energy $E_\mathrm{H}^{(i)}$, and the energies $E_\mathrm{D}^{(i,j)}$ due to dipolar interaction with particles $j \neq i$. For simplicity, a temperature independent uniaxial anisotropy is considered,

$$E_\mathrm{A}^{(i)} = -KV_i \left[\frac{\boldsymbol{\mu}_i \cdot \boldsymbol{n}_i}{|\boldsymbol{\mu}_i|} \right]^2, \tag{1}$$

where K denotes the anisotropy constant and the unit vector $\boldsymbol{n}_i$ denotes the orientation of the easy directions. The coupling to the applied field $\boldsymbol{H}$ is described by

$$E_\mathrm{H}^{(i)} = -\boldsymbol{\mu}_i \cdot \boldsymbol{H}, \tag{2}$$

and the energy due to magnetic dipolar interaction between particle i and particles $j \neq i$ located at $\boldsymbol{r}_i$ and $\boldsymbol{r}_j$ is given by

$$E_\mathrm{D}^{(i,j)} = \frac{\boldsymbol{\mu}_i \cdot \boldsymbol{\mu}_j}{r_{ij}^3} - \frac{3\,(\boldsymbol{\mu}_i \cdot \boldsymbol{r}_{ij})\,(\boldsymbol{\mu}_j \cdot \boldsymbol{r}_{ij})}{r_{ij}^5}, \tag{3}$$

where the inter-particle distance is $\boldsymbol{r}_{ij} = \boldsymbol{r}_i - \boldsymbol{r}_j$ and $r_{ij} = |\boldsymbol{r}_{ij}|$. Adding up the three terms given in equations (1–3) and summing over all particles, the system's total energy is obtained,

$$E = \sum_i E_\mathrm{A}^{(i)} + \sum_i E_\mathrm{H}^{(i)} + \frac{1}{2} \sum_i \sum_{j \neq i} E_\mathrm{D}^{(i,j)}, \tag{4}$$

as used in the MC simulations [25]. The samples considered in the following consist of $N = 125$ particles with identical volume $V_i = V$. The unitless concentration c is defined as the ratio between the total volume $\sum_i V_i = NV$ occupied by the particles and the sample volume V_sample, $c = \sum_i V_i / V_\mathrm{sample} = NV/V_\mathrm{sample}$. As this study focuses on the influence of the particle positions' disorder on the magnetic properties, the results discussed in the following are obtained for a constant moderate concentration $c/c_0 = 0.13$, where $c_0 = 2K/M_\mathrm{S}^2$ is a unitless material constant [26].

To perform the main MC simulation, a set of disordered particle positions $\{\boldsymbol{r}_i\}_\mathcal{C}$ and a set of randomly chosen orientations $\{\boldsymbol{n}_i\}_\mathcal{C}$ of the easy axes are needed for each configuration $\mathcal{C}$. To obtain the sets of disordered particle positions $\{\boldsymbol{r}_i\}_\mathcal{C}$ in a well-defined and controllable way, a preceding positional MC simulation is performed before the main magnetic MC simulation. During this preceding positional MC simulation [25], the particles can move freely in a cubic box of linear size $L^\star$ and interact only by a standard Lennard-Jones pair potential $v_\mathrm{LJ}^\star(r^\star) = 4[(1/r^\star)^{12} - (1/r^\star)^6]$ with periodic boundary

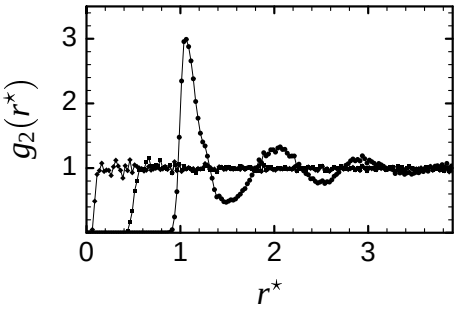

Fig. 1. Plot of the pair correlation function $g_2(r^\star)$ *vs.* $r^\star$ of the particle arrangement obtained by the preceding MC simulation, for $T^\star = 1$ (circles), 10^4 (squares), and 10^{12} (diamonds).

conditions (quantities with * indicate reduced variables of the preceding MC simulation). For the reduced density $\varrho^\star = N[L^\star]^{-3} = 0.85$ is chosen, and the system is thermalized for the desired reduced temperature $T^\star$. To rely specifically on the Lennard-Jones system to produce the particle positions is mainly motivated by the fact that it is well studied, for a detailed discussion see for example [27]. It is important to note that in the case under consideration the reduced temperature $T^\star$ is *not* a real physical temperature, but just provides a scalar parameter controlling the particle positions' disorder [28]. One way to characterize the resulting positional disorder is by obtaining the configurational averaged pair correlation function $g_2(r^\star)$, defined as

$$g_2(r^\star) = \left\langle \frac{1}{4\pi\varrho^\star N[r^\star]^2} \sum_{i,j \neq i} \delta(r^\star - r_{ij}^\star) \right\rangle_\mathcal{C}. \tag{5}$$

The pair correlation function $g_2(r^\star)$ is shown in Figure 1 for the three different values $T^\star$ used later on: $T^\star = 1$ and 10^4, which approximately cover the disorder being present in actual experiments (with $T^\star = 10^4$ being already a bit too large), and $T^\star = 10^{12}$, which is taken as an extreme value (see discussion below). For $T^\star = 1$, one obtains a liquid-like arrangement very similar to the one used in [23], with all particles well separated and no distances smaller than $r_\mathrm{min}^\star \cong 0.95$ present. For $T^\star = 10^4$ and $T^\star = 10^{12}$, the liquid-like pair correlations disappear, as $g_2(r^\star) = 1$ means no pair correlation, and the minimum distance is reduced to $r_\mathrm{min}^\star \cong 0.45$ and $r_\mathrm{min}^\star \cong 0.08$, respectively.

After the preceding MC simulation has provided the set of disordered particle positions $\{\boldsymbol{r}_i\}_\mathcal{C}$ for the current configuration $\mathcal{C}$, the respective orientations $\{\boldsymbol{n}_i\}_\mathcal{C}$ of the particles' easy axes are chosen randomly, and both the positions and the orientations remain constant during the following main magnetic MC simulation. The long-range dipolar interaction is treated with periodic boundary conditions using Ewald's summation for an infinite sphere surrounded by vacuum [27,29] (for an alternative MC approach based on effective field treatment see for example [30] and references therein). During the main MC simulation, the temperature T and the applied field H are changed as discussed below, and the magnetization M in the direction of the applied field is recorded in

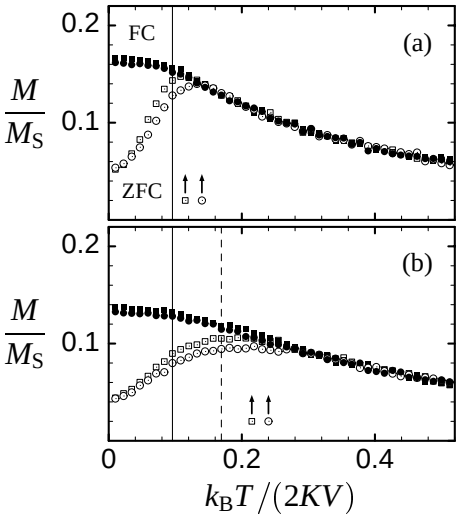

Fig. 2. Plot of the magnetization M/M_S *vs.* temperature $k_BT/(2KV)$ obtained by ZFC/FC with a cooling/heating rate of $k_B|\Delta T|/(2KV) = 0.01225$ every 8000 MC steps (open and full circles) and every 32,000 MC steps (open and full squares), for (a) $T^\star = 1$ and (b) $T^\star = 10^4$. The arrows indicate the respective blocking temperature T_B, and the error bars are about the size of the symbols. The temperatures $k_BT/(2KV) = 0.09575$ (full vertical line) and $k_BT/(2KV) = 0.16925$ (dashed vertical line) are marked, *cf.* Figure 4.

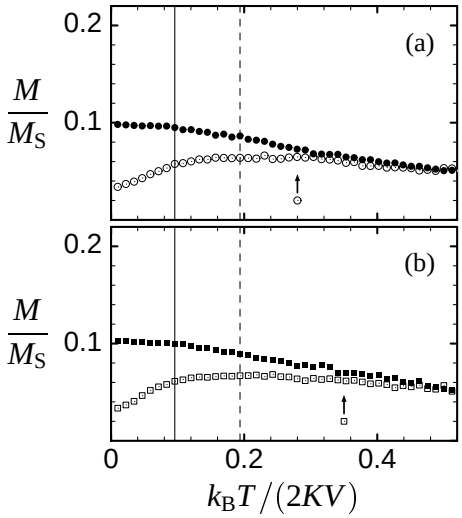

Fig. 3. Plot of the magnetization M/M_S *vs.* temperature $k_BT/(2KV)$ obtained by ZFC/FC with a cooling/heating rate of $k_B|\Delta T|/(2KV) = 0.01225$ every 8000 MC steps (open and full circles, shown in (a)) and every 32,000 MC steps (open and full squares, shown in (b)) for $T^\star = 10^{12}$. The arrows indicate the respective blocking temperature T_B, and the error bars are about the size of the symbols. The temperatures $k_BT/(2KV) = 0.09575$ (full vertical line) and $k_BT/(2KV) = 0.19375$ (dashed vertical line) are marked, *cf.* Figure 4.

certain time intervals (for further details concerning the application of the Metropolis MC algorithm [25] to the present model see [23,31]). The whole procedure of preceding MC simulation, randomly choosing the easy axes, and main MC simulation is repeated for each configuration $\mathcal{C}$, and an ensemble average is performed by averaging over more than 600 (when simulating ZFC/FC experiments) and 160 (when simulating long-time relaxation experiments) independent configurations.

3 Results

A first investigation of the systems characterized by the three different types of particle positions' disorder is done by performing simulations of ZFC/FC experiments. During such an experiment, the system is first demagnetized at high temperatures and cooled in zero field, afterwards a small field is applied, the system is heated until reaching (super-)paramagnetic temperatures (yielding the ZFC magnetization) and then cooled again (yielding the FC magnetization). For the applied field $H/H_A = 0.1$ is used in the present case, where $H_A = 2K/M_S$ denotes the anisotropy field, and the system is cooled and heated with two different constant rates of $k_B|\Delta T|/(2KV) = 0.01225$ every 8000 or 32,000 MC steps, respectively. The obtained magnetization M *vs.* temperature T is shown in Figures 2 and 3. First, one finds the rather unexpected result that the blocking temperature T_B depends crucially on the underlying particle positions' disorder, as the blocking temperature T_B for $T^\star = 10^4$ is almost twice as high as for $T^\star = 1$, *cf.* Figure 2. The blocking temperature T_B is defined here as the temperature where the respective ZFC and FC curves start to differ, and is indicated by arrows in the figures (concerning the microscopic relevance and other possible definitions of T_B see below). When (logarithmically) changing the value of $T^\star$ from 1 to 10^4, with this range approximately covering the disorder being present in actual experiments, the blocking temperature T_B changes smoothly and interpolates between the two values observed in Figure 2. The mechanism occurring at T_B is identical in both cases $T^\star = 1$ and 10^4 (as well as for the intermediate cases), as it can be seen when taking into account the influence of the cooling/heating rate. As it is apparent from Figure 2, the blocking temperature decreases when reducing the cooling/heating rate, and will approach zero at infinitely slow cooling/heating rate. Hence, in these two cases the system is driven out of equilibrium at a certain temperature that depends on the cooling rate (or analogously reaches equilibrium at the same temperature when heated), and a non-equilibrium blocking of the magnetic moments occurs at T_B.

This mechanism occurring at T_B for $T^\star = 1$ and 10^4 is completely different from the one present in the extreme case $T^\star = 10^{12}$ shown in Figure 3, where the opposite influence of the cooling/heating rate is observed. Here, the obtained blocking temperature T_B *increases* unambiguously when reducing the cooling/heating rate, which strongly indicates that there is not a non-equilibrium blocking but a cooperative freezing of the magnetic moments occurring at T_B. In difference to the cases $T^\star = 1$ and 10^4, the values of the magnetization obtained for $T^\star = 10^{12}$ applying the two different cooling/heating rates

differ slightly for the temperature range $k_{\rm B}T_{\rm B}/(2KV) < k_{\rm B}T/(2KV) \leq 0.5$, meaning that the systems are not (completely) in equilibrium for these temperatures above the blocking temperature $T_{\rm B}$ [32]. This observation leads to the important point concerning the microscopic relevance of the observed $T_{\rm B}$. In the cases $T^\star = 1$ and 10^4 shown in Figure 2, the distribution of the effective energy barriers is expected to be rather narrow, so that the *macroscopically* observed blocking temperature coincides with the average *microscopic* blocking temperature. In the extreme case $T^\star = 10^{12}$ shown in Figure 3, however, it is questionable whether this relation still holds, as cooperative effects are expected to be important and the distribution of the effective energy barriers will hence be very broad. As a result, some particles' magnetic moment may already be effectively frozen above the macroscopically observed blocking temperature $T_{\rm B}$ on the time scale given by the applied rate of temperature change, explaining the observed slight dependence of the magnetization on the cooling/heating rate in the temperature range above $T_{\rm B}$. Although other definitions of the macroscopic blocking temperature are possible and applied in literature (for example defining the blocking temperature as the temperature of the maximum of the ZFC curve), they all share inevitablely the problem that the obtained value cannot be directly related to the microscopic blocking temperatures being present in the system when the distribution of the effective energy barriers is very broad. Nevertheless, the blocking temperature $T_{\rm B}$, defined in one way or another, is still a macroscopic observable providing insight into the energy scale relevant in the system and is hence commonly used for good reasons to characterize samples in simulations as well as in actual experiments.

To further assess the validity of these results, for each of the three values of $T^\star$ four independent simulations of constant temperature relaxation experiments in the applied field $H/H_{\rm A} = 0.1$ are performed. The simulations differ by the field applied during cooling the system to the temperature $k_{\rm B}T/(2KV) = 0.09575$ well below the respective blocking temperatures $T_{\rm B}$ (*cf.* Figs. 2 and 3) with a rate of $k_{\rm B}|\Delta T|/(2KV) = 0.01225$ every 8000 MC steps: (i) cooling in zero field, (ii) cooling in the applied field $H/H_{\rm A} = 0.1$, and (iii) cooling in the saturated fields $H/H_{\rm A} = 4$ as well as (iv) $H/H_{\rm A} = -4$. When the desired temperature is reached, the applied field is changed to $H/H_{\rm A} = 0.1$ [cases (i), (iii), and (iv)] or remains at $H/H_{\rm A} = 0.1$ [case (ii)], respectively, and the relaxation starts. Shown in Figure 4 is the resulting magnetization M *vs.* elapsed time t (in number of MC steps). As the blocking temperatures $T_{\rm B}$ of the three investigated systems differ strongly, the conceptual problem arises for which temperature one should compare the relaxation behavior of the systems, as one can either compare for (α) given constant T or (β) given constant ratio $T/T_{\rm B}$. Therefore, in Figures 4b and c additionally shown are the results for the relaxation for the two cases (iii) and (iv) of cooling in saturated fields to the higher temperature $k_{\rm B}T/(2KV) = 0.16925$ (Fig. 4b) and $k_{\rm B}T/(2KV) = 0.19375$ (Fig. 4c), which both have

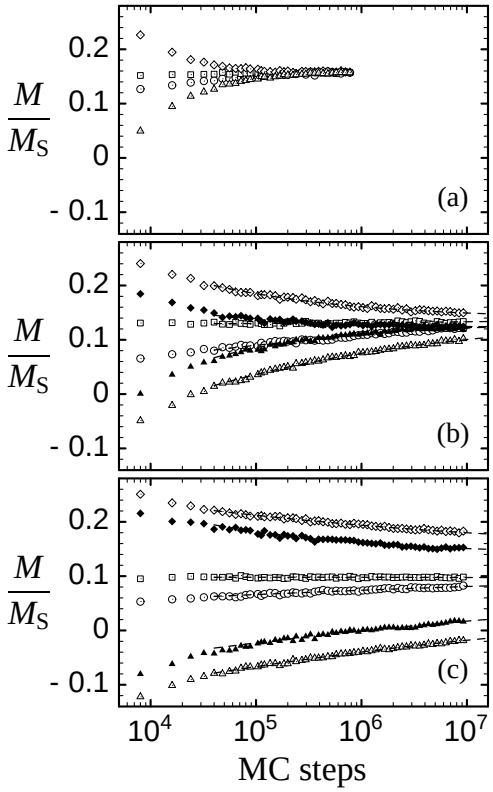

Fig. 4. Plot of the magnetization $M/M_{\rm S}$ *vs.* time t (in number of MC steps) for applied field $H/H_{\rm A} = 0.1$ and for (a) $T^\star = 1$, (b) $T^\star = 10^4$, and (c) $T^\star = 10^{12}$. The open symbols correspond in all three cases to the temperature $k_{\rm B}T/(2KV) = 0.09575$, whereas the closed symbols correspond to the temperature (b) $k_{\rm B}T/(2KV) = 0.16925$ and (c) $k_{\rm B}T/(2KV) = 0.19375$. The different symbols indicate (i) cooling in zero field (circles), (ii) cooling in the applied field $H/H_{\rm A} = 0.1$ (squares), and cooling in the saturated fields (iii) $H/H_{\rm A} = 4$ (diamonds) and (iv) $H/H_{\rm A} = -4$ (triangles). The dashed lines shown in (b) and (c) indicate the fits $M = M_0 + M_1 t^{-\alpha} \log_{10} t$, *cf.* text. The error bars are about the size of the symbols.

the same ratio $T/T_{\rm B} \cong 0.69$ as the value $k_{\rm B}T/(2KV) = 0.09575$ used in Figure 4a. From Figures 4a and b one can estimate that for $T^\star = 1$ and 10^4 the involved relaxation times are of the order of 10^5 and 10^7 MC steps at the fixed temperature $k_{\rm B}T/(2KV) = 0.09575$, and of the order of 10^5 and 10^6 MC steps at the fixed ratio $T/T_{\rm B} \cong 0.69$. The increase from $T^\star = 1$ to 10^4 slows down significantly the relaxation (both for fixed T and for fixed ratio $T/T_{\rm B}$), and hence the positional disorder has a large influence on the system dynamics, confirming the results obtained by the ZFC/FC simulations. Nevertheless, an equilibrium value of the magnetization exists in both cases and is reached within experimental time scale, thus further supporting the conclusion that one observes non-equilibrium blocking of the magnetic moments at $T_{\rm B}$.

In the extreme case $T^\star = 10^{12}$, however, one again encounters a completely different behavior, *cf.* Figure 4c. The observed values of the magnetization are distinct after 10^7 MC steps, and furthermore the data shows a pronounced curvature. Thus, the relaxation becomes slower

than $\log_{10} t$ before the values of the magnetization coincide, and the magnetization seems to level off at distinct values which depend on the sample history. As no analytical form of the relaxation is known, the data for $t \geq 4 \times 10^4$ MC steps is fitted using the ansatz $M = M_0 + M_1 t^{-\alpha} \log_{10} t$ with the obtained exponents α ranging from $\alpha = 0.1$ to 0.4, shown as dashed lines in Figure 4c. The above conclusion of distinct long-time values for the magnetization is supported by the fact that these fits which take into account the curvature do *not* intersect *nor* merge for $t \to \infty$, pointing towards the non-existence of an equilibrium value of the magnetization. (It is important to note that analogous fits of the data shown in Fig. 4b *do* intersect and merge.) Ignoring the existing curvature and fitting the data shown in Figure 4c using the worst case linear form $M = M_0' + M_1' \log_{10} t$, one finds intersections at approximately 10^{11} MC steps for both temperatures shown, which is 6 orders of magnitude larger than the relaxation times for $T^\star = 1$ and far beyond what is accessible numerically. Although based on the current results one is not able to definitely exclude relaxation towards and hence the existence of an equilibrium value of the magnetization, this relaxation has to occur on a time scale logarithmically larger than 10^{11} MC steps. Furthermore, the very large energy barriers needed for such long relaxation times to occur can only be explained by cooperative effects being present in the system. Thus, the system with $T^\star = 10^{12}$ shows a cooperative freezing at T_B by any practical measure.

4 Conclusions

In summary, the particle positions' disorder has been identified as a crucial parameter having a large influence on the low temperature behavior of systems of dipolarly interacting single-domain ultrafine ferromagnetic particles, in accordance with recent experimental observations [22]. For values of positional disorder covering the range being present in actual experiments, $T^\star = 1$ and 10^4, a non-equilibrium blocking of the magnetic moments occurs at T_B. Evidence has been given that for extreme values of positional disorder, $T^\star = 10^{12}$, the simple model studied can even show a cooperative freezing at low temperatures, and it might be interesting to study quantities such as the non-linear susceptibility to further support the current results and to definitely prove the existence of a spin glass phase [33]. However, it is important to stress that this presumable spin glass behavior occurs in any case for parameter values which are not realized in the experiments for which spin glass behavior has been reported. The reason is that for a given volume concentration c there is a maximal value of $T^\star_\mathrm{max}$ which can be realized in actual experiments, with $T^\star_\mathrm{max}$ increasing for decreasing volume concentration c. For values of $T^\star$ larger than $T^\star_\mathrm{max}$, the particles' minimal interdistance, which decreases with increasing $T^\star$, will get smaller than the particles' diameter, which of course cannot occur in actual experiments. As the volume concentration in the model system can only be given as multiple of the material constant c_0, for example $c/c_0 = 0.13$ as in this study [26], the results for $T^\star = 10^{12}$, besides being interesting from a theoretical point of view, might nevertheless be relevant for hypothetical systems of ultrafine ferromagnetic particles which have a small value of c_0, *i.e.* a small anisotropy constant K and/or a large saturation magnetization M_S. In any case, the important conclusion is that, in spite of the large influence the positional disorder has on the magnetic properties of single-domain ultrafine ferromagnetic particles, it cannot serve to explain the experimentally observed spin-glass behavior. So the question what causes the spin glass behavior in the experiments reported so far remains open.

References

1. J.L. Dormann, D. Fiorani, E. Tronc, Adv. Chem. Phys. **98**, 283 (1997).
2. E.C. Stoner, E.P. Wohlfarth, Phil. Trans. Roy. Soc. A **240**, 599 (1948) [reprinted in IEEE Trans. Mag. **27**, 3475 (1991)].
3. L. Néel, Ann. Geophysique **5**, 99 (1949).
4. W.F. Brown, Phys. Rev. **130**, 1677 (1963).
5. A. Aharoni, I. Eisenstein, Phys. Rev. B **11**, 514 (1975).
6. W.T. Coffey, D.S.F. Crothers, Yu.P. Kalmykov, E.S. Massawe, J.T. Waldron, Phys. Rev. E **49**, 1869 (1994).
7. S. Shtrikman, E.P. Wohlfarth, Phys. Lett. A **85**, 467 (1981).
8. R.W. Chantrell, E.P. Wohlfarth, J. Magn. Magn. Mater. **40**, 1 (1983).
9. J.L. Dormann, L. Bessais, D. Fiorani, J. Phys. C **21**, 2015 (1988).
10. R.W. Chantrell, M. El-Hilo, K. O'Grady, IEEE Trans. Mag. **27**, 3570 (1991).
11. W.L. Luo, S.R. Nagel, T.F. Rosenbaum, R.E. Rosensweig, Phys. Rev. Lett. **67**, 2721 (1991).
12. S. Mørup, E. Tronc, Phys. Rev. Lett. **72**, 3278 (1994).
13. S. Mørup, Europhys. Lett. **28**, 671 (1994).
14. T. Jonsson, J. Mattsson, C. Djurberg, F.A. Khan, P. Nordblad, P. Svedlindh, Phys. Rev. Lett. **75**, 4138 (1995).
15. J.L. Dormann, F. D'Orazio, F. Lucari, E. Tronc, P. Prené, J.P. Jolivet, D. Fiorani, R. Cherkaoui, M. Noguès, Phys. Rev. B **53**, 14291 (1996) and J.L. Dormann, L. Spinu, E. Tronc, J.P. Jolivet, F. Lucari, F. D'Orazio, D. Fiorani, J. Magn. Magn. Mater. **183**, L255 (1998).
16. M.F. Hansen, F. Bødker, S. Mørup, K. Lefmann, K.N. Clausen, P.-A. Lindgård, Phys. Rev. Lett. **79**, 4910 (1997).
17. C. Djurberg, P. Svedlindh, P. Nordblad, M.F. Hansen, F. Bødker, S. Mørup, Phys. Rev. Lett. **79**, 5154 (1997).
18. C. Johansson, M. Hanson, M.S. Pedersen, S. Mørup, J. Magn. Magn. Mater. **173**, 5 (1997).
19. M.F. Hansen, S. Mørup, J. Magn. Magn. Mater. **184**, 262 (1998).
20. H. Mamiya, I. Nakatani, T. Furubayashi, Phys. Rev. Lett. **80**, 177 (1998).
21. T. Jonsson, P. Svedlindh, M.F. Hansen, Phys. Rev. Lett. **81**, 3976 (1998).

22. M.F. Hansen, C.B. Koch, S. Mørup, Phys. Rev. B **62**, 1124 (2000).
23. J. García-Otero, M. Porto, J. Rivas, A. Bunde, Phys. Rev. Lett. **84**, 167 (2000).
24. G. Ayton, M.J.P. Gingras, G.N. Patey, Phys. Rev. Lett. **75**, 2360 (1995); Phys. Rev. E **56**, 562 (1997); S. Ravichandran, B. Bagchi, Phys. Rev. Lett. **76**, 644 (1996); Phys. Rev. E **54**, 3693 (1996); for a comprehensive review on orientational glasses see U.T. Höchli, K. Knorr, A. Loidl, Adv. Phys. **39**, 405 (1990).
25. All MC simulations (the preceding positional and the main magnetic one) are performed using the standard Metropolis algorithm, see for example K. Binder, D.W. Heermann, *Monte Carlo Simulations in Statistical Physics: An Introduction*, Springer Series in Solid State Science, Vol. 80, 3nd edn. (Springer, Berlin, 1997).
26. To give an estimate for the concentration $c/c_0 = 0.13$ in real units: Maghemite particles with mean diameter around 7.5 nm studied by Jonsson *et al.* [14] show $M_S = 420$ emu/cm^3 and $K = 1.9\times10^5$ erg/cm^3, which gives $c_0 \cong 2.15$. For iron-nitride particles with mean diameter around 6 nm, Mamiya *et al.* [20] found $M_S = 1182$ emu/cm^3 and $K = 10^6$ erg/cm^3, which yields $c_0 \cong 1.43$. Accordingly, the concentration $c/c_0 = 0.13$ considered corresponds to $c \cong 0.28$ in the case of maghemite particles and to $c \cong 0.18$ in the case of iron-nitride particles.
27. M.P. Allen, D.J. Tildesley, *Computer Simulation of Liquids* (Clarendon Press, Oxford, 1987).
28. In an actual experiment, the effective $T^\star$ may be controlled for example by the particles' coating, *cf.* Ref. [22].
29. S.W. de Leeuw, J.W. Perram, E.R. Smith, Proc. R. Soc. Lond. A **373**, 27 (1980).
30. A.F. Pshenichnikov, V.V. Mekhonoshin, J. Magn. Magn. Mater. **213**, 357 (2000); R.W. Chantrell, N. Walmsley, J. Gore, M. Maylin, Phys. Rev. B **63**, 024410 (2001).
31. J. García-Otero, M. Porto, J. Rivas, A. Bunde, J. Appl. Phys. **85**, 2287 (1999) and J. García-Otero, M. Porto, J. Rivas, J. Appl. Phys. **87**, 7376 (2000).
32. However, it is important to stress that the systems are heated high enough into the equilibrium (super-)paramagnetic state up to the maximal temperature $k_BT_{max}/(2KV) = 1$, so that it is guaranteed that the system is in thermal equilibrium before the FC part starts. This is verified by additional simulations of relaxation experiments for $k_BT/(2KV) = 1$ starting with samples equilibrated in saturated fields $H/H_A = -4$ and $H/H_A = 4$. Both systems relax towards a common value of the magnetization, which conincides with the one obtained by ZFC/FC simulations, in less than 3×10^3 MC steps after changing the field to $H/H_A = 0.1$.
33. See for example K.H. Fischer, J.A. Herz, *Spin Glasses* (Cambridge University Press, Cambridge, 1991).